

GIS TECHNIQUES FOR MAPPING URBAN VENTILATION, USING FRONTAL AREA INDEX AND LEAST COST PATH ANALYSIS

M. S. Wong^a, J. E. Nichol^a, E. Y. Y. Ng^b, E. Guilbert^a, K. H. Kwok^a, P. H. To^a, J. Z. Wang^a

^a Department of Land Surveying and Geo-Informatics, The Hong Kong Polytechnic University
Kowloon, Hong Kong

^b School of Architecture, The Chinese University of Hong Kong

m.wong06@fulbrightmail.org

Commission VI, WG VI/4

KEY WORDS: Frontal area index, Landscape roughness parameter, Least cost path analysis, Wind ventilation

ABSTRACT:

This paper presents the urban wind ventilation mapping from building frontal area index on the example of urbanised city, Hong Kong. The calculations of frontal area index for each uniform 100m grid cell are based on three dimensional building databases at eight different wind directions. The frontal area index were then correlated with land use classification map, and the results indicate that commercial and industrial areas were found to have higher values as compared to other urban land use types, primary because these areas have densely high rise buildings. However, with using the frontal area index map, the potential ventilation paths created using least cost path analysis of the city can be located, and the “in-situ” measurements were suggested the existence and accuracy of these ventilation paths. These high ventilation paths could play significant roles in relieving the urban heat island formation and increasing the urban wind ventilation, planning and environmental authorities may use the derived frontal area index and ventilation maps as objective measures of environmental quality over a city, especially human comfort of the urban climate.

1. INTRODUCTION

Most of the data included in wind and air quality studies are from ground level instrument. The gathering of data over large regions therefore is a major challenge to these studies. Wind tunnel model provides an alternative for visualizing the local wind direction and pollutant dispersion in a large scale over a city. Duijm (1996) experimented the wind tunnel model in Lantau island of Hong Kong in a large scale (1:4000) of a small area. Mfula et al. (2005) tested the pollution sources affect by buildings and analysed the wind and pollutant patterns of the surface, a very large building model scale at 1:100. Although wind tunnel studies of air ventilation in urban can provide accurate datasets of concentration fields, measured under hypothesis and constrained conditions, the small coverage, computer demanding requirements and high operational cost are prohibitive its usage. In recent years, a variety of numerical models has been developed for modelling air ventilation, such as PSU/NCAR mesoscale model (known as MM5) and Computational fluid dynamics (CFD) model. The MM5 model works for mesoscale phenomena such as air flow of sea breeze and mountain-valley flow (Dudhia et al., 2003) with large coverage and at coarse resolution, while the CFD model simulates urban wind flow at a larger scale. The CFD model is being widely used in engineering flow analysis, building and structural design, urban wind flow predictions (Baik and Kim, 1999), and air pollution dispersal modelling (Blocken et al., 2007; Huber et al., 2004; Kondo et al., 2006). The CFD model comprises a set of physical models which attempt to closely match the real geometry inside the urban areas and thus simulate the air flow. This model is highly site-specific and

cannot be used for all meteorological conditions eg. other cities. Fine resolution products achieve higher accuracy are mainly used for monitoring at street and district levels, due to the higher computational requirements. Therefore, any task of wind ventilation model at city-scale, over densely urbanised regions with complex street and building structures will become more challenging.

However, GIS and remote sensing techniques then provide solutions with simplifying assumptions and numerical approximations. Wind modelling at near surface condition can always be simplified mathematically through the estimating of roughness parameters. There are many studies on modelling and retrieving surface roughness using GIS and remote sensing techniques, and several methods and parameters have been suggested on calculation of surface roughness: zero-plane displacement height (z_d) and the roughness length (z_0) (Lettau, 1969; Counihan, 1975), plan area density (λ_p), frontal area index (λ_f) (Grimmond and Oke, 1999; Burian et al., 2002), average height weighted with frontal area (z_h), depth of the roughness sub-layer (z_r) (Bottema, 1997; Grimmond and Oke, 1999) and the effective height (h_{eff}) (Matzarakis and Mayer, 1992) etc.

Among these urban morphological parameters, frontal area index is suggested as a good indicator for mesoscale meteorological and urban dispersions models (Burian et al., 2002). Frontal area index is the measurement of building walls facing the wind flow in a particular direction (frontal area per unit horizontal area) (Figure 1). It has a strong relationship with surface roughness z_0 , and as a function with flow regime inside

urban street canyons (Burian et al., 2002). More details of frontal area index will be illustrated in section 3.

The aim of this paper is to (i) analyse the frontal area index with different land use classification types in Hong Kong. (ii) In further, the occurrence frequency of ventilation paths generated from Least Cost Path (LCP) analysis over the study area was used to gain insights to the high ventilation locations, and prevailing transport pathways of airflow. The technique described provides high resolution raster maps which has more understanding on wind ventilation and its interactions with different geometries of buildings at city-scale. (iii) The validity of the mapped ventilation paths was then evaluated in the field with “in-situ” measurements. The deliverables are the maps of frontal area index and the maps of occurrence frequency of ventilation paths.

2. STUDY AREA

The Kowloon peninsula in Hong Kong was selected for the study. It consists of high-density residential areas, financial and commercial districts, and urban parks. The population within the study area is approximately 2 million. The topography is flat in the southern part and hilly terrain is located in the northern part where the elevation has a range from 3m to 300m.

3. METHODS

3.1 Calculation of frontal area index

The frontal area index (λ_f) is calculated as the total areas of building facets projected to plane normal facing the particular wind direction divided by the plane area (Equation 1).

$$\lambda_f = A_{\text{facets}} / A_{\text{plane}} \quad (1)$$

where λ_f is the frontal area index, A_{facets} is the total areas of building facets facing the wind direction, and A_{plane} is the plane area.

Burian et al. (2002) used a similar approach for estimating the λ_f in Los Angeles. Here we modified the algorithm by eliminating the blocking areas facing the wind direction on the blocked buildings. Figure 1 illustrates an example of frontal area calculation. Those areas of facets on second buildings were not calculated. A program was written in ESRI® ArcGIS™ 9.2 software to estimate the total frontal areas in the projected plane normal to specific wind direction using digital data of building polygons from the Hong Kong Lands Department. The scale of the digital data is 1:5000. This program was first screened for particular wind direction and generated projected lines with 5m increment horizontally. If the projected lines hit the first facet and could not reach the second facet, only the frontal area of the first facet would be calculated. This process is important for irregular building groups and can reduce number of facets being calculated in computer memory. A splitting process was then applied to ensure building groups were split into individual buildings, and all building polygons were inside their corresponding plane polygons.

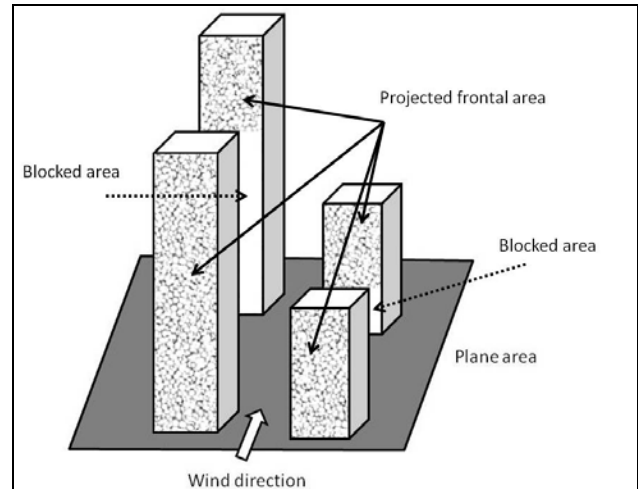


Figure 1. Example of frontal area calculation

For the plane area, we divided the study area into grid cells of 100m x 100m size. Nichol and Wong (2008) show that the resolution at 200m may indicate intra-urban differences at meso-scale between different land cover types but smaller areas such as green spaces with ca. 1 hectare (100m²) can produce significantly lower surface temperature in urban areas. In addition, the Planning Department (2009) in Hong Kong also found that grid resolution at 100m was compatible to all variables in determining dynamic potential and thermal load contributions in urban climatic study. Thus, our study calculated λ_f at 100m grid resolution in a large 11km by 7km urban area, for eight different wind directions (north, northeast, east, southeast, south, southwest, west, and northwest).

3.2 Frontal area index in different land use types

In Hong Kong, as in most cities, different land use types support different building structures and characteristics, for example: high-rise buildings (>50 floors) in residential, 20-30 floorers in commercial districts, and 20-50 storey larger buildings in industrial district. Therefore, it was expected that these areas would have different λ_f properties. This study used a generalized land use map at 10m resolution acquired from the Hong Kong Planning Department for analysing the relationship between λ_f and different land use.

3.3 Ventilation paths: least cost path analysis

In order to evaluate the relevance of frontal area index to the fresh air corridors in the study area, Least Cost Path (LCP) analysis was undertaken to compare those pathways generated in different wind directions. The pathways represent routes of “high potential” of ventilation locations in the city, degree of connectivity between starting and ending points, and minimum Euclidean distance by considering the cumulative pixel values at each grid cell. The rationale of LCP is to identify the path of least resistance across a cost surface from a starting point to an ending point. This study adopted an approach by allocating variable weightings to the frontal area index of each pixel, eg. the higher λ_f , the higher the friction value. The friction values represent the percentage of obstruction of wind ventilation or air flow, these values can be varied according to the user.

First, the λ_f map was imported to IDRISI v.14.02 (Clark Labs., Worcester, MA, USA). The λ_f pixel values were reclassified into 5 classes and each class was given a weight as friction

value. Table 1 shows the weights assigned to 5 classes. Second, starting points should be given, for example, there are fifty points allocated on the east coast of Kowloon peninsula representing the eastward wind transporting across the peninsula from east to west. The friction surface was then created by the IDRIS COST module which computes cost surfaces for the fifty starting points. Third, fifty ending points allocated on the west coast of Kowloon peninsula were then input to the PATHWAY module (Eastman, 2006) for generating LCPs. Finally, there are 2500 and 5186 LCPs for eastward and northeastward wind respectively (Figure 3). The occurrence frequencies for the grid cells in the study domain are calculated by counting the overlaid of LCP segments. Thus, grid cells with high occurrence frequencies are associated with the low friction values, and these cells are indicated as areas of “high potential” contribution of wind ventilation. All these processes were implemented in customization scripts in IDRISI, and the results are shown in section 4.3.

Allocated friction value	λ_f
20	<0.2
40	0.2-0.4
60	0.4-0.6
80	0.6-0.8
100	>0.8

Table 1. Friction values allocated to different classes of λ_f

4. RESULTS

4.1 Map of λ_f

Figure 2 shows the gross distribution of averaged λ_f in eight directions over study area. For the general downtown area, typical average of λ_f is 0.25. Isolated high buildings (>400m high) can be found near the west coast of Kowloon peninsula. It is one of the claims for causing “wall effect” which blocks the sea-breeze wind transporting into the downtown, thus inducing significant UHI effect.

Since the most densely built areas are devoid of vegetation, and elsewhere street planting is severely restricted by lack of space (Jim, 2004), urban vegetation is small and fragmented. Since urban vegetation has a small frontal area comparatively to artificial buildings, trees are not considered in the λ_f calculation. In addition, the urban topography in mainly is flat, terrain is also not considered.

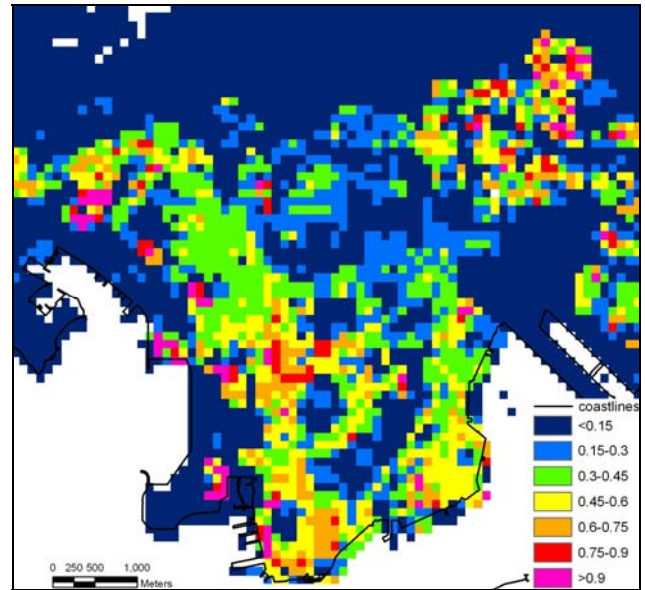


Figure 2. Map of frontal area index

4.2 Relationship between λ_f and different land use types

Table 2 shows the λ_f as a function of different land use types. The industrial and commercial types have the significant high λ_f (0.324 and 0.305) compared to the others. Residential classes have moderate high λ_f (~0.254), public transportation and warehouse have lower λ_f (~0.15). A direct relationship between the frontal area index and the building characteristics can be demonstrated in this study since a general trend can be observed with higher λ_f always associated with wider and taller buildings (eg. industrial and commercial districts). Burian et al. (2002) found that the λ_f in residential, commercial, industrial, public transportation are 0.176, 0.246, 0.095, 0.011 respectively in Los Angeles. Grimmond and Oke (1999) studied the λ_f in major cities in north America, and they found the highest λ_f in city center in Vancouver, Canada (0.3) and suburban residential areas in Arcadia, United States (0.33). Although a direct comparison between our study and the others cannot be made due to different algorithms for calculating λ_f , we can still note that the urban areas in Kowloon peninsula have significantly high λ_f values.

Landuse types	λ_f
Private Residential	0.267
Public Residential	0.241
Commercial/Business & Offices	0.305
Industrial	0.324
Warehouse & Storage	0.155
Rural Settlements	0.056
Vegetation	0.075
Public transportation	0.15
Vacant Development Land	0.191

Table 2. Friction values allocated to different classes of λ_f

4.3 Ventilation paths

The eastward and northeastward λ_f maps gave somewhat similar results (Figure 3a, 3c), but different on the distributions of occurrence frequency of LCPs (Figure 3b, 3d). In Figure 3b and

3d, the cross and triangle symbols represent the starting and ending points of the LCPs. There are a total of 2500 and 5186 segments created from easterly and northeasterly directions. From the distribution of the occurrence frequency of LCPs, one can see that the “high potential” of easterly wind ventilation paths are mostly located on

(i) Boundary street (marked as A in Figure 3b). The route traverses between residential area with low-rise buildings across patches of vegetated areas. This street is a marked boundary between the southern and northern Kowloon, where the southern part was ceded to the United Kingdom in 1860 and the northern part was leased in 1898. The occurrence frequency of LCPs along this route is greater than 30% (750/2500).

(ii) Argyle street and Cherry street (marked as B in Figure 3b). This is the shortest route, but is a four-lane dual-way which connects the old airport in the east to the west coast. This route provides significant air corridor in east-west direction and the occurrence frequency of LCPs along this route is greater than 18% (450/2500).

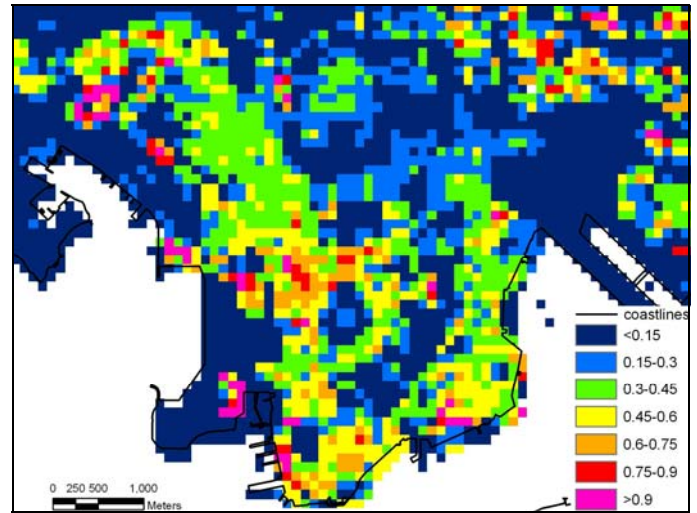
(iii) Ho Man Tin Hill road, King’s park road and Gascoigne road (marked as C in Figure 3b). This route traverses large patch of urban vegetation, low density residential development with fragmented trees, and densely commercial areas. The occurrence frequency of LCPs along this route is only greater than 16% (400/2500) which is the least among three.

For these routes, flows are from the east and reached the new reclamation land in the west. These three routes are generally represented by occurrence frequency greater than 24%. However, the northeasterly wind ventilation path is located on

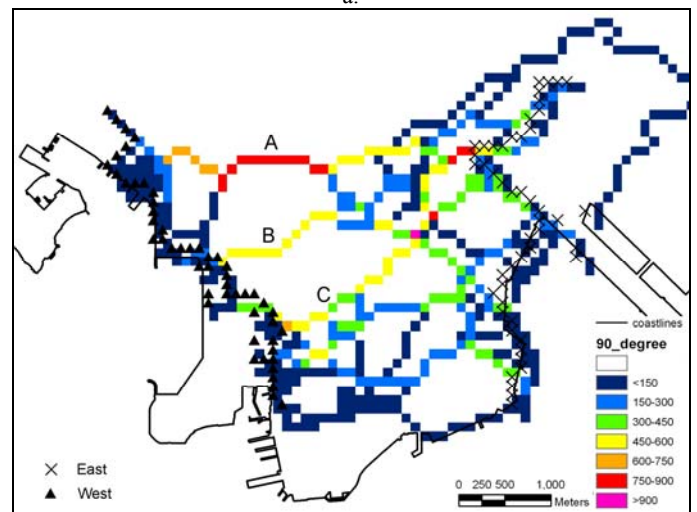
(iv) Princess Margaret road, Chatham road, Hong Chong road and Salisbury road (marked as D in Figure 3d). This route comprises of low rise residential area, urban park, university campus, commercial district and harbor walkway. Route D is the only significant route contains segments in north-south direction among all the 5186 paths. From this route, air flow is from the northeast to the south and turned westerly along the south coast of peninsula. This route is represented by occurrence frequency greater than 28% (1500/5186).

These four air flow pathways had the “higher potential” wind ventilation locations and accounted for the greater number of LCP segments. However, since the easterly and northeasterly winds dominate 66% of all the wind directions in Hong Kong, the north-south oriented street and building geometry reinforce the trapping of polluted air at the downtown. Due to the wind blocking by ridged mountains (eg. 900m height) on the north of peninsula, the fresh air corridors in north-south direction are rarely observed. This study only observes a significant segment of route D in north-south direction.

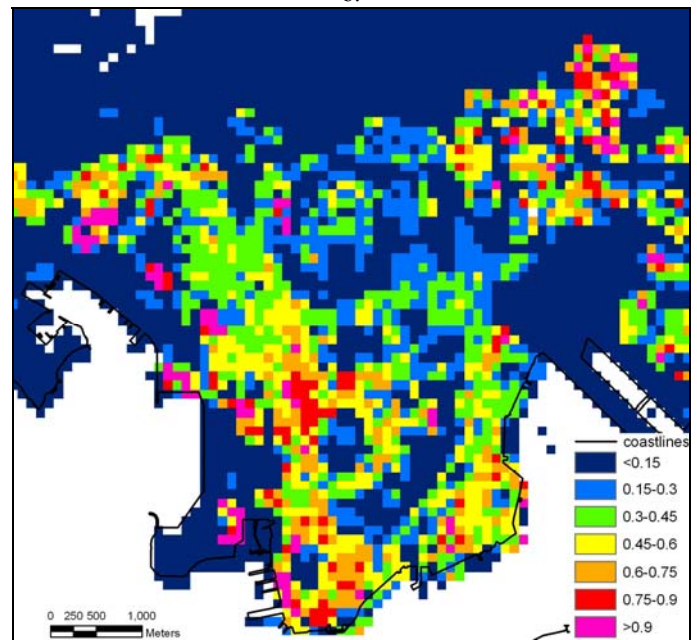
These maps of ventilation paths facilitate the visualization of wind ventilation and show the specific locations in the city e.g. those in red and purple colours, which appear to provide potential air flow corridors for dispersing of the urban pollution. These maps therefore promote better understanding of air ventilation at detailed, as well as in city scale.



a.



b.



c.

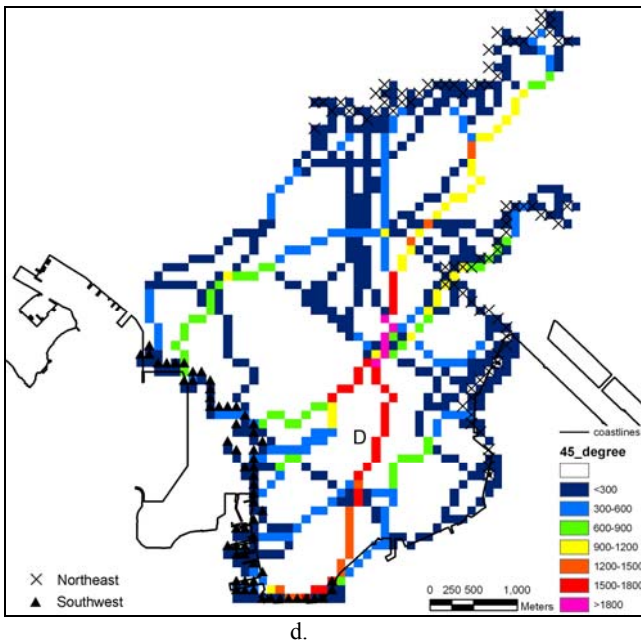


Figure 3. a. Frontal area index map in east-west direction; b. Occurrence frequency of ventilation paths in east-west direction (total number of paths is 2500); c. Frontal area index map in northeast-southwest direction; b. Occurrence frequency of ventilation paths in northeast-southwest direction (total number of paths is 5186)

4.4 Validation strategy

In order to investigate the significance and functionality of the occurrence frequency of ventilation paths, fieldwork was undertaken on 09 Oct 2009, 13 Oct 2009, 15 Oct 2009. The general wind direction of these days are 45, 90, 45 degree, respectively. A slow walk was undertaken along the differing sections of the route A and D, recording the wind speed and locations by GPS along the routes. The wind speeds were measured on 4 occasions, and the results are averaged. These two routes were only chosen because their high occurrence frequencies of ventilation paths, and the total number of “in-situ” measurements along route A and D are 22 and 48 respectively. Figure 4 shows the “in-situ” measurements overlaid with occurrence frequency of ventilation paths, the dots’ sizes represented the “in-situ” measurement are scaled with the wind speed. Along the route A, average and maximum wind speeds were observed with values of 9.3m/s and 17.8m/s respectively, and the background wind speed was 2m/s. The wind speed off the route was remarkably low (ca. 2.3m/s). About 55% of “in-situ” data with wind speed larger than 9.1m/s fall in the higher occurrence frequency of 24%, and about 32% of data with wind speed larger than 5.7m/s fall in moderate occurrence frequency of 18%. This may be indicated that route A is identified as a key connecting corridor link the air in the eastern and western sections of the peninsula. However, along route D, the average and maximum wind speeds are smaller than route A, they are 3.5m/s and 12.4m/s respectively. The background wind speed is 0.65m/s and that off the route is ca. 1.1m/s. Approximate 44%, 25% and 21% of data fall in higher occurrence frequencies of 28%, 23%, 17% respectively. However, the largest wind speed (12.4m/s) was observed on the harbor walkway on the south coast of peninsula, since the wind was not only from the north at that location, the sea breeze and offshore wind apparently were the source resulted in this high

wind speed. In this validation study, the analysis of occurrence frequency of ventilation paths provided what appears to provide more realistic information on wind speeds and air corridors over the city, especially significantly ventilation paths are observed on route A and D. Since the model has potential for pinpointing the key buildings and refining the building geometry for better air ventilation, this can be useful for urban redevelopment and land reclamation.

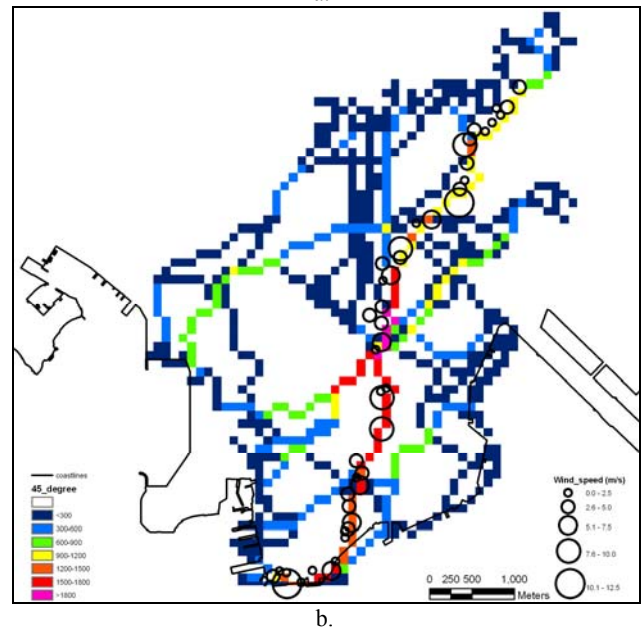
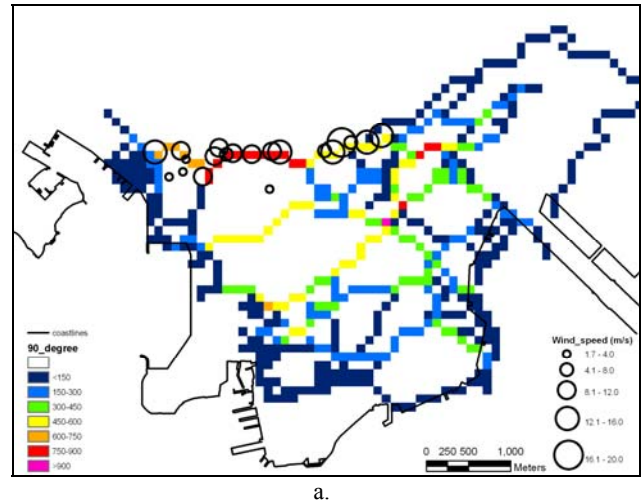


Figure 4. Occurrence frequency of ventilation paths overlaid with “in-situ” measurements in a. east-west direction, b. northeast-southwest direction

5. CONCLUSION

This paper presents a comprehensive study of urban ventilation using the model of roughness parameter - building frontal area index on the example of a large urban area in Hong Kong. We calculated the frontal area index based on three dimensional building data under a refined algorithm, as a function of land use type. Most of the frontal area indices as a function of land use type were found to be similar to values computed for other studies, but commercial and industrial areas were found to have

significantly high values because these areas are high rise in Hong Kong.

To evaluate the air ventilation in city scale over Hong Kong, LCP analysis was performed. However, whereas LCP analysis usually operates with single segment on purpose, this study adopted an innovative approach by overlaid the LCP segments to derive maps of occurrence frequency of LCP. Four major air ventilation pathways were identified from these maps. The pathways, routes A, B, C, D accounted for 30%, 18%, 16%, 24% respectively of all least cost paths, and they pass from easterly and northeasterly directions respectively. "In-situ" wind speeds were measured to evaluate the robustness and accuracy of the models, and the results apparently show consistency between modelled pathway and "in-situ" measurements.

In densely urbanised Hong Kong, resolution corridors of 100m width in this study may not appear to provide viable connecting corridors at street level, but it would be sufficient for city scale modelling. This study offers a more complete and relevant air ventilation study, and such detailed mapping at city scale has not been undertaken previously. The fuzzy querying on assigning the weights of friction values to the frontal area index pixels can be varied to facilitate upscaling to coarser resolution for regional scale study, eg. regional air dispersion model or wind ventilation models. However, given the high accuracy and high spatial resolution of deriving the wind ventilation model for a city, planning and environmental authorities may use the derived maps as an objective measure of air quality and wind ventilation over a whole city, for comparisons between places and cities and for monitoring changes over time.

Acknowledgments

The authors would like to acknowledge the Hong Kong Planning Department for land use and Tertiary Planning Unit data, and the Hong Kong Lands Department for building GIS databases. This project was funded by PolyU SURF project 1-ZV4V.

References

Baik, J.J. and Kim J.J., 1999. A numerical study of flow and pollutant dispersion characteristics in urban street canyons. *Journal of Applied Meteorology*, 38, pp. 1576–1589.

Blocken B., Carmeliet J. and Stathopoulos T., 2007. CFD evaluation of the wind speed conditions in passages between buildings – effect of wall-function roughness modifications on the atmospheric boundary layer flow. *Journal of Wind Engineering and Industrial Aerodynamics*, 95(9-11), pp. 941-962

Bottema, M., 1997. Urban roughness modelling in relation to pollutant dispersion. *Atmospheric Environment*, 31, pp. 3059-3075.

Burian S.J., Brown M.J. and Linger S.P., 2002. Morphological analysis using 3D building databases, Los Angeles, CA. LA-UR-02-0781, Los Alamos National Laboratory, USA.

Counihan J., 1975. Adiabatic atmospheric boundary layers: a review and analysis of data from the period 1880–1972. *Atmospheric Environment*, 9, pp. 871–905.

Dudhia J., Gill D., Manning K., Wang W. and Bruyere C., 2003. PSU/NCAR Mesoscale modeling system tutorial class notes and user's guide: MM5 modeling system version 3, NCAR.

Duijm N.J., 1996. Dispersion over complex terrain: wind-tunnel modelling and analysis techniques. *Atmospheric Environment*, 30(16), pp. 2839-2852.

Eastman R., 2006. IDRISI Andes Tutorial, Clark Labs, Worcester, USA.

Grimmond C.S.B. and Oke T.R., 1999. Aerodynamic properties of urban areas derived from analysis of surface form. *Journal of Applied Meteorology*, 34, pp. 1262–1292.

Huber A.H., Tang W., Flowe A., Bell B., Kuehlert K. and Schwarz W., 2004. Development and applications of CFD simulations in support of air quality studies involving buildings. 13th Joint Conference on the Applications of Air Pollution Meteorology with the Air & Waste Management Association, (CD-ROM) Vancouver, British Columbia, Canada, August 23-27, 2004.

Jim C.Y., 2004. Impacts of intensive urbanisation on trees in Hong Kong. *Environmental Conservation*, 25(2), pp. 146-159.

Kondo H., Asahi K., Tomizuka T. and Suzuki M., 2006. Numerical analysis of diffusion around a suspended expressway by a multi-scale CFD model. *Atmospheric Environment*, 40, pp. 2852-2859.

Lettau H., 1969. Note on aerodynamic roughness-parameter estimation on the basis of roughness-element description. *Journal of Applied Meteorology*, 8, pp. 828–32.

Matzarakis A. and Mayer H., 1992. Mapping of urban air paths for planning in Munchen. *Wissenschaftliche Berichte Institut for Meteorologie und Klimaforschung*, The University of Karlsruhe, 16, pp. 13–22.

Mfula A.M., Kukadia V., Griffiths R.F. and Hall D.J., 2005. Wind tunnel modelling of urban building exposure to outdoor pollution. *Atmospheric Environment*, 39(15), pp. 2737-2745.

Nichol J.E. and Wong M.S., 2008. Spatial variability of air temperature over a city in a winter night. *International Journal of Remote Sensing*, 29(24), pp. 7213-7223.

Planning Department, 2009. Urban Climatic Map and Standards for Wind Environment - Feasibility Study. January 2009.